J Mater Sci (2010) 45:1725–1733
DOI 10.1007/s10853-009-4133-0

Study on silicon carbide nanowires produced from carbon blacks and structure of carbon blacks

M. Wieligor · R. Rich · T. W. Zerda

Received: 9 July 2009 / Accepted: 16 December 2009 / Published online: 6 January 2010

Abstract Silicon carbide nanowires were produced from carbon blacks at 1473 K and their microstructure was characterized by TEM, X-ray diffraction, FTIR and Raman spectroscopy. Nanowires of uniform diameters, the smallest averaging 10 nm, and narrow size distribution were obtained from graphitized carbon blacks, and their morphology depends on the properties of carbon black precursors. High concentration of stacking faults and twins was detected. In addition to silicon carbide nanowires, a silicon carbide layer, about 20 nm thick, was formed on the surface of carbon black aggregates. The interior of the aggregates did not react and analysis of the data showed that it is composed of a mixture of amorphous carbon and small graphitic crystallites. The small lateral sizes of these crystallites remain unchanged during the graphitization process which is limited to the outer layer of the aggregates.

Introduction

Silicon carbide nanowires are usually produced by the vapor–liquid–solid process; however, the yield is very small [1, 2]. Previously we have demonstrated that silicon carbide nanowires can be produced in large quantities from carbon nanotubes and silicon powder under vacuum conditions at temperatures around 1500 K [3, 4]. We found that diameters of SiC nanowires depend on the sizes of carbon nanotubes, sintering temperature, and the duration of the reaction. SiC exists in the form of different polytypes, the most common being cubic (3C) and hexagonal (2H and 6H). However, our nanowires are all of cubic 3C symmetry. The low energy of planar faults formation in SiC results in high concentration of those defects in the nanowires as well as in bulk material [3].

SiC has many interesting properties including very high melting temperature, 3000 K, low thermal expansion coefficient, 4×10^{-6} K^{-1}, good thermal conductivity, 85–260 W/mK [5], high hardness, $H = 27$ GPa, and high fracture toughness, 4.6 MPa $m^{1/2}$ [6]. It is a semiconductor, and its large band gap, 2.2–3.2 eV for various polytypes, makes it an attractive candidate for electronic devices operating at high temperatures [7, 8]. Recently, another possible application has been discovered—graphene layers have been found to grow on SiC surface [9, 10].

Large volume production of SiC nanowires from carbon nanotubes is expensive, thus requiring the need for alternate manufacturing methods utilizing more economical precursors. In this paper, we report results on silicon carbide nanowires obtained from carbon blacks. Carbon blacks are inexpensive and readily available in various sizes and morphologies. Shapes of carbon black aggregates and the size of particles constituting the aggregates depend on the operational conditions of the reactor, among which temperature distribution within the flames, degree of turbulence in the gas flow, speed of the gasses, and residence time before water quenching are considered most important [11]. Although the shapes and sizes of the aggregates vary widely, dimensions of graphitic nanocrystallites detected within the particles are similar for all raw carbon blacks, about 2 nm in lateral size [11]. Post-production heat treatment of carbon blacks results in extensive graphitization manifested by increased crystallite sizes. In the past,

M. Wieligor · R. Rich · T. W. Zerda (✉)
Department of Physics and Astronomy, Texas Christian University (TCU), Box 294480, Fort Worth, TX 76129, USA
e-mail: t.zerda@tcu.edu

we have studied this process using Raman spectroscopy, X-ray diffraction, neutron scattering, gas adsorption, and transmission electron microscopy [12–15]. Our results show that in carbon blacks graphitized at 3000 K, the lateral sizes of graphitic crystallite reach 6 nm for low grades of carbon blacks, N100 and N200 series, 14 nm for N660, and 23 nm for N990 [14]. In the next section, we discuss the experimental procedure and characterize silicon carbide structures obtained from these various carbon black sources.

Experimental

Carbon blacks were obtained from Sid Richardson Carbon Co., and they were washed in toluene and dried prior to experiments. The graphitization process was conducted in an induction furnace. Selected carbon blacks, N234, N660, and N990, were each heat treated for at least 10 min at 1273, 2273, and 3000 K. Silicon powder of maximum grain size 30 nm was obtained from Aldrich.

Silicon and the carbon reactants were not mixed but placed at the opposite ends of 10 cm long quartz ampoules. Next, the ampoules were evacuated, sealed, and heated to 1473 K. The reaction time was set to 52 h. Silicon sublimed and its vapor reacted with carbon to form silicon carbide. The presence of silicon carbide was verified by X-ray diffraction, FTIR and Raman spectroscopy. X-ray diffractograms were obtained on a Philips diffractometer with copper K_α radiation, $\lambda = 1.54$ Å.

Infrared spectra were obtained using a Nexus 650 from Thermo Nicolet. Small amounts of specimens were mixed with KBr and pressed into pellets. The resolution was 4 cm^{-1}.

Raman spectra were obtained using a microimaging system consisting of a solid state laser operating at 514 nm wavelength, an Olympus BH2 microscope, and a transmission dispersive spectrometer from Kaiser equipped with a CCD detector. Spectral resolution was 4 cm^{-1}, and the laser power at the surface of the sample varied from 10 to 100 mW. To avoid laser burning of dark samples, the specimens were pressed into a grove of a disk which rotated with a speed of about 4000 rpm, thus preventing the burning effects. The spectra were obtained with 3 min exposure times and were analyzed using Grams software. Some spectra were obtained with a 785 nm laser and then the spectral resolution was about 8 cm^{-1}.

Transmission electron microscopy (TEM) images were obtained using JEOL 2100 system with the accelerating voltage of 200 kV. EDS spectra were obtained using an EDAX detector.

SEM images were obtained on an FEI-XL30 system. Magnification ranged from 1000 to 100,000×.

Results

Several different grades of carbon blacks were used in this study, but we will focus our discussion on only three: N234, N660, and N990.

N234

The X-ray diffractograms of the specimen obtained from N234 showed only SiC peaks (see Fig. 1). The TEM images of the specimen after the reaction with silicon (Fig. 2b) showed structures similar to the carbon black aggregates observed in the raw N234 (Fig. 2a), but the high-resolution TEM images and the EDS analysis clearly showed that after the reaction the aggregates were not carbon black but fused SiC spheres. Furthermore, the analysis of high-resolution TEM images (inset in Fig. 2b) indicated that silicon carbide aggregates were wrapped up with a thin layer of amorphous silicon carbide, less than 2 nm thick. In addition to the SiC aggregates, we also noticed the presence of SiC nanowires (Fig. 3). These

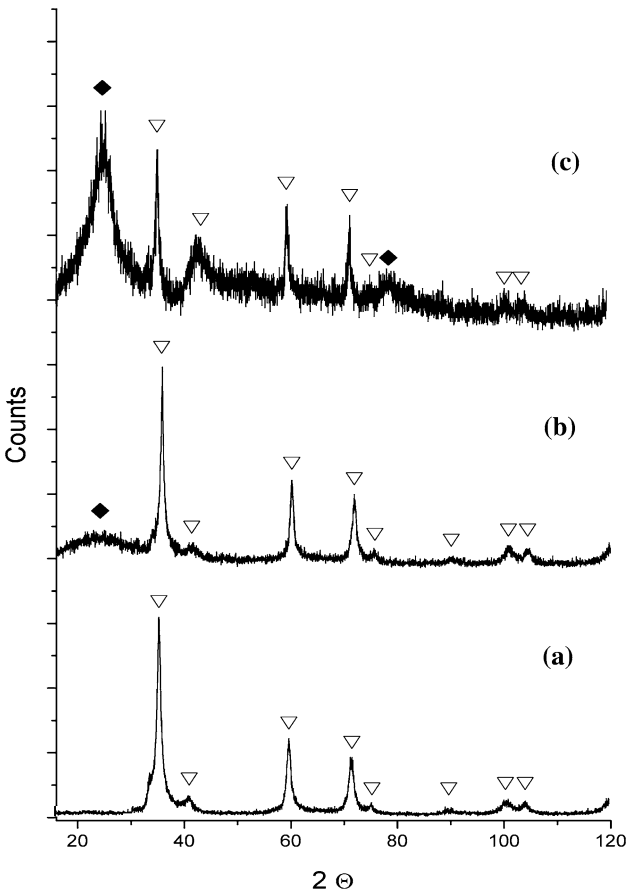

Fig. 1 X-ray diffractograms of specimens obtained from N234 (**a**); N660 (**b**); and N990 (**c**). *Open triangles* show peaks due to silicon carbide and *filled diamonds* due to carbon black

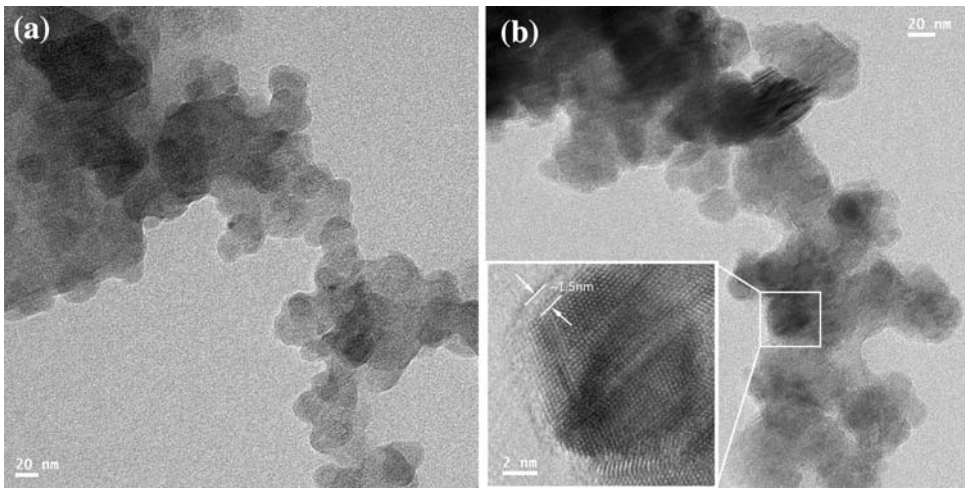

Fig. 2 TEM images of carbon black aggregates in raw N234 before the reaction (**a**) and after the reaction with Si (**b**). The inset depicts a high resolution image of several crystallites in an aggregate. Amorphous layer around the aggregates can be seen

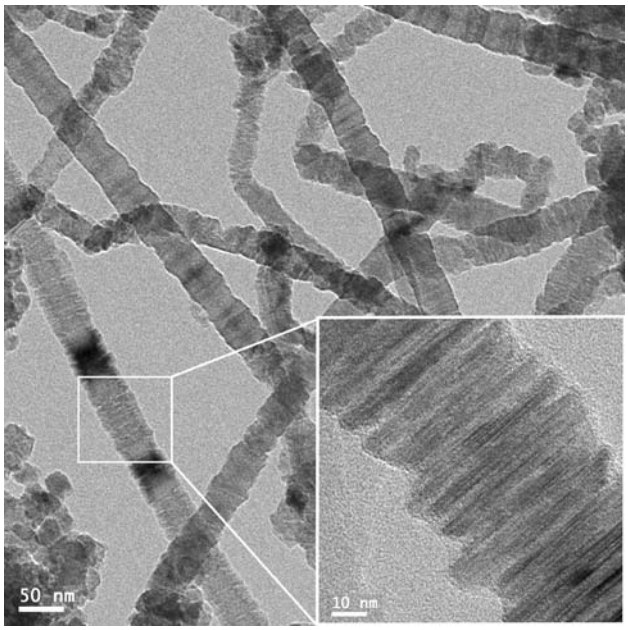

Fig. 3 SiC nanowires obtained from N234. The inset shows structure of a section of one wire

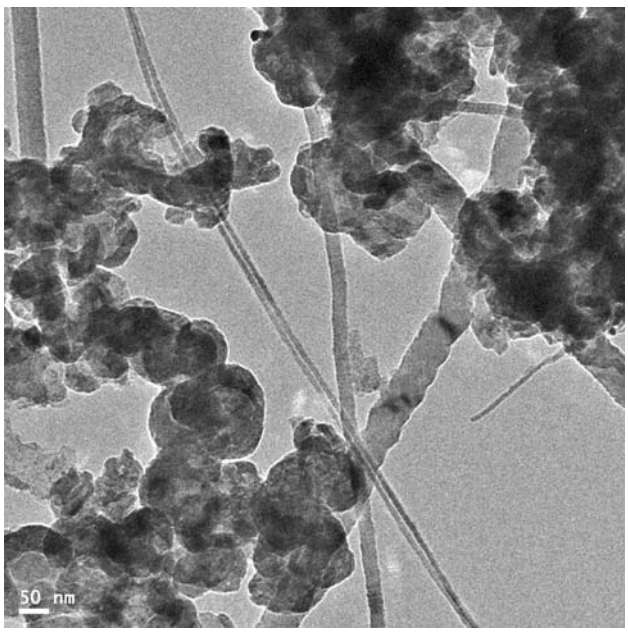

Fig. 4 A typical TEM image of the specimen obtained from N660. SiC is present in the form of fused aggregates and long nanowires

wires had diameters ranging from 10 to 70 nm and lengths from 250 nm to 2 μm.

N660

After the reaction with silicon, in all TEM images of N660, an example is presented in Fig. 4, we can clearly see SiC aggregates and SiC nanowires.

Contrary to the reaction with N234, the reaction with N660 was partially complete and in addition to SiC, X-ray diffractograms indicated also the presence of a small amount of graphite (see Fig. 1b). We did not quantify the concentration of graphite in those specimens, but from X-ray diffractograms it appears that in the sample obtained from graphitized N660 there is more graphite than in the specimen obtained from the raw N660. Raman spectra (Fig. 5) confirmed this result. The two peaks characteristic for SiC, one at 790 cm^{-1}, the TO mode, and another at 938 cm^{-1}, the LO mode, were accompanied by the 1580 and 1355 cm^{-1} doublet, a characteristic feature for graphite. In addition, we observed a band at about 860 cm^{-1} which has been assigned to Frohlich transitions enhanced by structural defects [16]. The peak at about 1580 cm^{-1} is the ordered peak of graphite, *G*, while the peak at 1355 cm^{-1} is the so-called disordered peak, *D*. The intensity ratio of the ordered and disordered graphite peaks were used to estimate lateral sizes of graphitic crystallites [17]

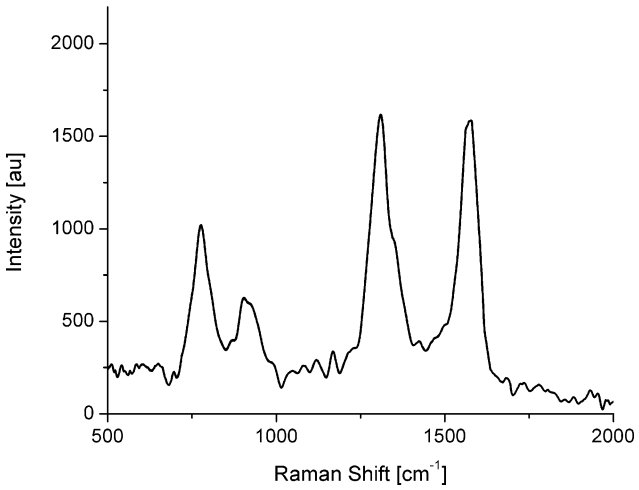

Fig. 5 Raman spectrum of the specimen obtained from N660. The peaks at 790 and 938 cm^{-1} are SiC TO and LO modes, while the peaks at 1580 and 1355 cm^{-1} are graphite ordered, *G*, and disordered, *D*, vibrations. Excitation line 785 nm

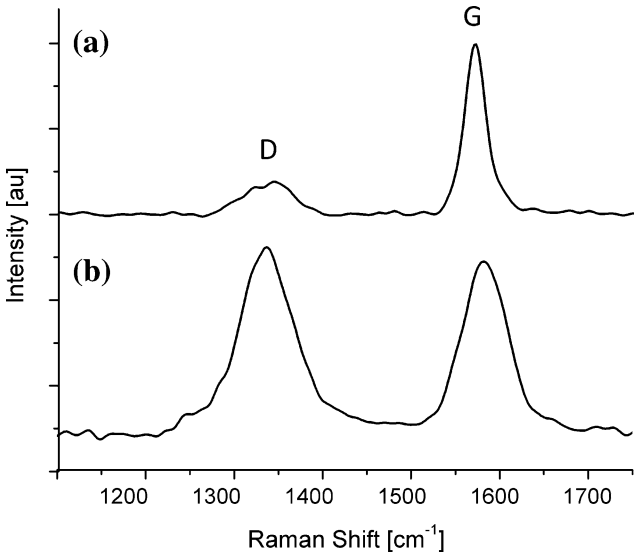

Fig. 6 Raman spectrum of a specimen obtained from N660 depicting two graphitic peaks, one organized, *G*, and another disorganized, *D*, centered at 1580 and 1355 cm^{-1}, respectively. The *top spectrum* was obtained immediately after the reaction with silicon; the *bottom spectrum* was obtained after the specimen was burned at 1000 K in air for 2 h. Excitation 514 nm laser

$$L_a = 43.5 I_D / I_G \quad (1)$$

where I_D and I_G are the intensities of the *D* and *G* peaks, respectively. After heating that sample in oxygen atmosphere for 2 h at 1000 K, the intensities of the graphitic peaks decreased substantially (compare Fig. 6). The calculated crystallite sizes, L_a, are listed in Table 1.

Table 1 Average lateral sizes (L_a) of the crystallites

Carbon black grade	L_a (nm) raw CB	L_a (nm) graphitized CB	L_a (nm) CB after the reaction with Si
N234	2.7	6.3	No carbon black left
N660	2.9	13.8	1.5
N990	2.5	23.5	1.7

N990

Particles present in carbon black N990 have average diameters of about 250 nm. These large particles, regardless of their history of heat treatment prior to the reaction with silicon, did not completely react with silicon. Therefore, X-ray diffractograms of the sintered products showed peaks characteristic of the SiC cubic 3C phase as well as those due to graphite (see Fig. 1c). Raman spectra also showed bands due to graphitic structures and SiC, similar to those depicted for specimens obtained from N660 (compare Figs. 5 and 6). After heating that sample in oxygen atmosphere for 2 h at 1000 K, the intensities of the graphitic peaks decreased substantially. Since Raman spectra of such burned specimens still showed peaks due to graphitic structure, we concluded that not all of the graphitic carbon was burned.

A TEM image of N990 after its reaction with silicon and heat treatment in air at 1000 K is shown in Fig. 7. A number of broken SiC shells of thickness of about 20 nm can be identified. In addition to SiC-coated spheres and empty shells, we have also observed regions with a high concentration of thin wires, an example is depicted in Fig. 8.

We measured diameters of the nanowires and then fitted experimental data to log-normal distribution functions. These functions obtained for selected carbon blacks are depicted in Fig. 9.

FTIR spectra of the products of the reaction between carbon blacks and silicon are similar, and an example is depicted in Fig. 10. In addition to the SiC phonons at 830 and 950 cm^{-1}, we detected a peak due to Si–O vibrations at about 1100 cm^{-1} and CH_x peaks at about 2900 cm^{-1} (not shown).

Discussion

Carbon blacks

Examination of TEM images recorded after the SiC coated N990 were burned at 1000 K revealed the presence of

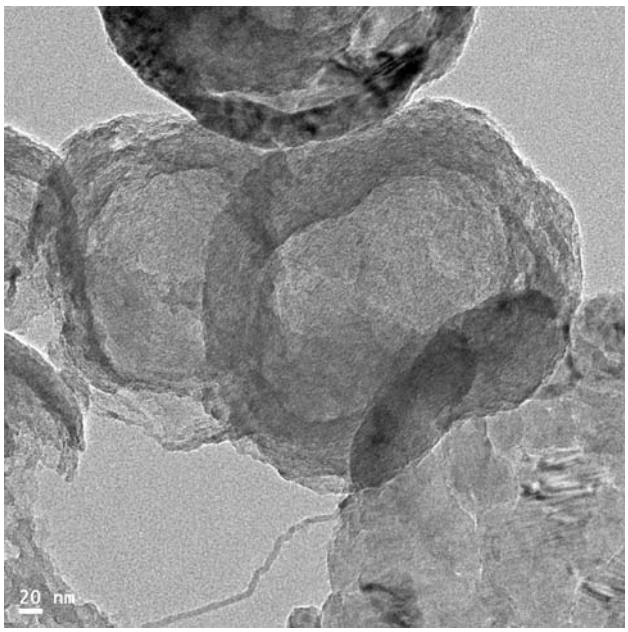

Fig. 7 A TEM image of SiC shells after the specimen obtained from N990 was heated to 1000 K for 2 h. The shells have shapes similar to those of carbon black aggregates. Fragments of broken shells can be easily identified. A single nanowire attached to an aggregate can be seen in the lower central part of the image

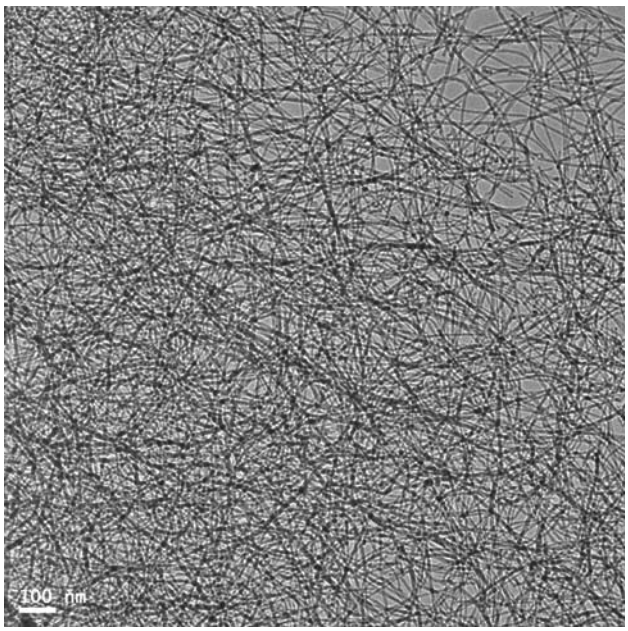

Fig. 8 An example of SiC nanowires obtained from graphitized N990. The lengths of these nanowires are measured in microns

small SiC fragments as well as hollow SiC shells. Of course, the majority of particles was not damaged and maintained the shapes of particles prior to the reaction with silicon. Obviously, these particles were completely coated with the SiC layer that prevented oxygen from reaching

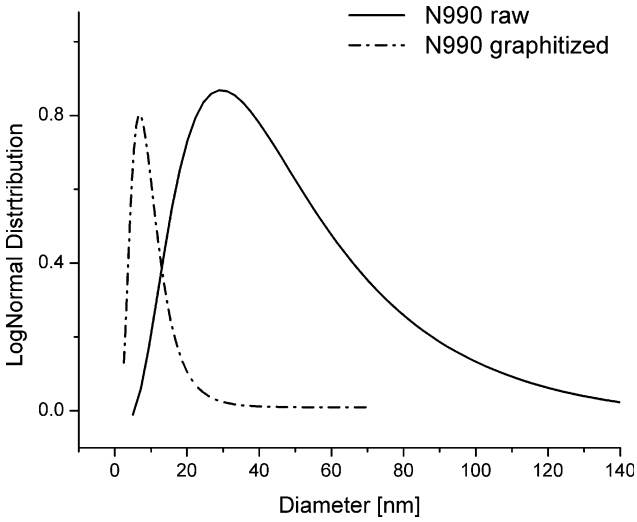

Fig. 9 Size distributions for SiC nanowires obtained from raw and graphitized N990. The *lines* show the log-normal distribution functions best fitted to the diameters measured from TEM images, such as shown in Fig. 8

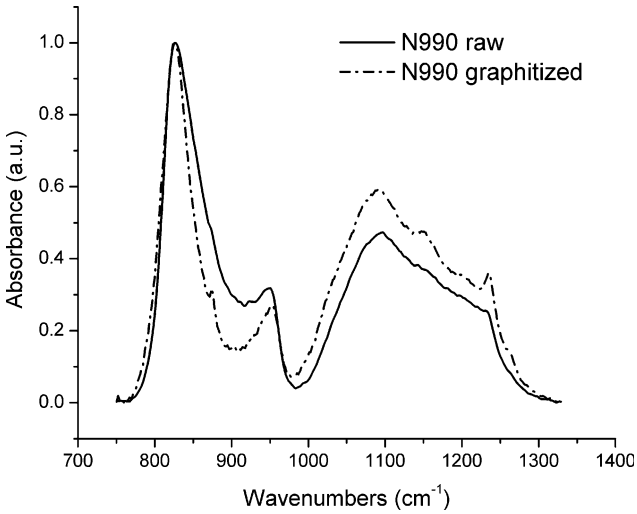

Fig. 10 FTIR spectra of raw and graphitized N990 after the reaction with silicon

carbon below that layer. But when the SiC shell was not complete or there was even a small crevice present, then oxygen reacted with the core and produced gases that broke the outer shell. The fragments of the shells were about 20 nm thick; therefore, we assumed that the SiC shell around the aggregates was of similar thickness.

A distance of about 4 cm separated both reactants in an evacuated ampoule. The reaction can proceed through two channels. Silicon vapor can directly react with carbon to form SiC, or oxygen released by quartz heated to a high temperature can form silicon oxide which readily reacts with carbon or carbon oxide to form SiC [1, 17]. When temperature of the ampoule increased to about 1000 K,

silicon started to sublime and silicon vapors filled out the ampoule. Of course, vapor pressure of silicon increases with increasing temperature, and for this reaction we chose $T = 1473$ K. Within less than 1 h, a thin layer of silicon carbide was formed on the surface of carbon blacks. For the reaction to continue, silicon and carbon atoms had to diffuse through that freshly created layer, and thus this stage of the reaction was controlled by the diffusion rates of silicon and carbon atoms in SiC. Reaction time was set to 52 h for all samples, and in the case of the N234 sample this time was enough for almost all carbon atoms to react and form SiC. The average radius of N234 particles is about 10 nm and the reaction time was sufficiently long to allow silicon and carbon atoms to diffuse through silicon carbide from the center of the particle to its surface [3]. On the other hand, larger particles contain more carbon atoms, and the silicon carbide layer could potentially be as thick as the particle radius. However, the thickness of the SiC layers formed on the larger particles in N990 or N660 were estimated from the TEM to be no more than 20 nm, which is smaller than the particle radius. Clearly, with growing thickness of the SiC film, the flux of reactants decreased, and 52 h was not long enough to completely convert large diameter carbon black particles into silicon carbide spheres. Consequently, the interior of these particles remained unchanged. Indeed, both X-ray diffractograms and Raman spectra showed signatures typical for both SiC and graphite (see Figs. 1, 5 and 6).

Raman spectra of carbon blacks N660 and N990 coated with SiC were obtained and used to calculate from Eq. 1 the average lateral sizes of the crystallites. These values were all similar and equal to about 1.5 nm. They are listed in Table 1 along with the corresponding values for carbon blacks prior to the reaction. Even for products obtained from carbons graphitized at 3000 K, the L_a values of graphitic structures present inside the particles were also very low. For these samples, Raman spectra originated from graphitic structures present inside the particles and below the SiC layer. We also concluded that carbon blacks graphitized at 3000 K had their outer surfaces graphitized while the interior was pretty much disorganized. Specifically, after the reaction with silicon, Raman spectra of products obtained from graphitized and raw N990 and N660 were similar; we concluded that both specimens had interiors with similar degree of disorder. This conclusion is in agreement with the results of neutron scattering study conducted by Hjelm et al. [18]. During graphitization, only the outer layers became organized while the centers of the particles remain unchanged.

The morphology of the products of the reaction was similar to the morphology of carbon blacks used in the manufacturing process. This conclusion is independent of carbon black grade or the degree of graphitization prior to the reaction. Particles of graphitized carbon blacks do not have round perimeters, as seen under high-resolution TEM. Their forms can be approximated by polygonal shapes, and the same morphology was found after the reaction. However, the edges of SiC coated aggregates were not as sharp as in the carbon black precursors (compare Figs. 2 and 7).

Interestingly, for the graphitized carbon blacks, the amount of unreacted carbon, estimated from X-ray diffraction pattern and Raman peak intensities, was greater than for the raw counterparts. The sizes of the aggregates did not change during graphitization of carbon blacks. Graphitization results in reduced surface concentration of amorphous carbon and the growth of large crystallites. Apparently, the diffusion rates of atoms were reduced in better organized structures. It is well established that the diffusion rates along the boundaries between crystallites or in crystallites with large concentration of defects are greater than those for the defect-free crystallites [19]. In raw carbon blacks, small crystallites create extended boundaries through which atoms can diffuse faster than through defect-free crystallites.

For the SiC layer to be formed on carbon black aggregates, carbon atoms needed to diffuse to the outer surface of that layer. It is possible that silicon diffused in the opposite direction; however, its diffusion rate in SiC is less than that of carbon [20, 21]. This process is too slow to explain the rate of SiC growth and we assume that the diffusion proceeds not through bulk crystals but through grain boundaries. The activation energies for grain boundary diffusion are about 40% lower than those for the bulk diffusion [19]. In our experiments, the grain boundaries account for a significant fraction of the sample volume, and atoms residing in grain boundaries, which may have thickness of about 0.5 nm, define the effective diffusivity.

Silicon carbide nanowires

Small diameter nanowires were observed in all TEM images recorded for various carbon black grades (Figs. 2, 4 and 8). In many respects, SiC nanowires produced from carbon blacks have similar structures as the nanowires which were obtained from carbon nanotubes and graphite. Therefore, we will briefly summarize main conclusions of SiC nanowires obtained from carbon nanotubes [3] and graphite [22] in this paragraph. These nanowires have the core–shell structure with the crystalline core of the cubic symmetry and the shell consisting of amorphous silicon carbide. The amorphous layer on SiC nanowires produced from carbon nanotubes was 5 to 10 nm thick. The presence of a thick amorphous layer is a common property of SiC nanowires obtained from many precursors and using different manufacturing techniques. For example, large

amorphous layers were reported for SiC nanowires obtained from SiO_2 and nanosize carbon particles [23], nanowires obtained by the thermal decomposition of ethanol in the presence of iron catalyst [24] or synthesized from polyacrylonitrile nanofibers [25]. In each of these cases, the thickness of the amorphous layer is larger than the size of SiC crystalline core. In our previous experiments involving carbon nanotubes, we obtained the smallest diameter SiC nanowires from multiwall carbon nanotubes of 30 nm average diameter sintered at 1500 K for 1 h. Larger diameter nanowires were obtained when either larger carbon nanotubes were used, the reaction time was extended, or the reaction temperature was increased. In the case of HOPG graphite, 10 nm nanowires were produced, but the yield was small [22]. Production of nanowires of controlled and uniform diameters is important for possible practical applications and this problem was addressed by many authors. Below we will report a few selected results. 10 nm nanowires were obtained without metal catalysts by Zhang et al. [23]. Slightly thicker nanowires, 23 nm, were manufactured by Kim et al. [24], or Ye et al. [25] who obtained 30 nm wires from 120 nm carbonized polyacrylonitrile fibers. Bogart and coworkers [26] used alumina templates and obtained SiC nanowires of controlled sizes ranging from 40 to 180 nm depending on the pore sizes in the alumina matrix. Control of diameters of SiC nanowires synthesized by carbothermal reduction of resorcinol-formaldehyde/SiO_2 aerogels is a difficult task and nanowires of sizes ranging from 10 to 150 nm were produced [27].

The EDS analysis of SiC nanowires produced from carbon blacks showed that their chemical composition was only Si and C. We did not detect even traces of metals. From the TEM images we measured the *d*-spacing between the crystallographic planes to be 2.52 Å, the value which indicated that the nanowires grew along the [111] direction. The nanowires had diameters which depended on the carbon black grade and the history of its heat treatment. From Fig. 9 it is seen that wires obtained from the graphitized N990 had the smallest diameters and a very narrow distribution. N234 yielded nanowires of a wide distribution, and the thickest wires obtained from graphitized N234 approached 120 nm in diameter. The lengths of nanowires produced from N234 varied widely from nanometers to microns, with the average value of about 1 μm. Also, some of these nanowires had diameters that changed along the cylinder axis, in one case from 24 to 18 nm across the distance of 30 nm.

Morphology of the nanowires depended on carbon black grades. The nanowires obtained from the tread grade carbon blacks, such as N110 and N234, had rough structures and some looked like building blocks stacked on the top of each other (see Fig. 3). Although the surface is rough, porosity of the nanowires is negligible as reflected by almost identical adsorption and desorption nitrogen isotherms. This is not a typical result; for example, Li et al. [28] reported porous SiC nanowires. The average height of these blocks was about 5 nm and were poorly aligned along the growth axis. Dark streaks visible in Figs. 3, 4 and 7 represent planar faults. Numerous twins were identified in the TEM images as regions with distinctly different crystallographic alignment forming an angle of 141° (see Fig. 11). Such structures were first observed by Shim and Huang [2].

It appears that stacking faults and twins are always present in SiC nanowires, regardless of the manufacturing technique and precursors used. However, the density of stacking faults and twins appears to be dependent on the diameter of the wires. This conclusion is similar to that reached by Zhang et al. [23], Niu et al. [29] and Roy et al. [28]. It is worth to note that our nanowires do not have lamellar twins extending down the length of the nanowires. Such structures were observed by Davidson and coworkers [30].

All nanowires formed from N660 and N990 had smooth outer surfaces and diameters that did not vary along their lengths. Twinning faults were abundant. As seen in Fig. 7, the silicon carbide wire originated on the surface of the particle and the size of that nanowire corresponds to the size of the surface crystallite.

The fact that graphitized N234 produced nanowires of sizes ranging from 10 to 120 nm can be explained in terms of the growth of these nanowires that originated from

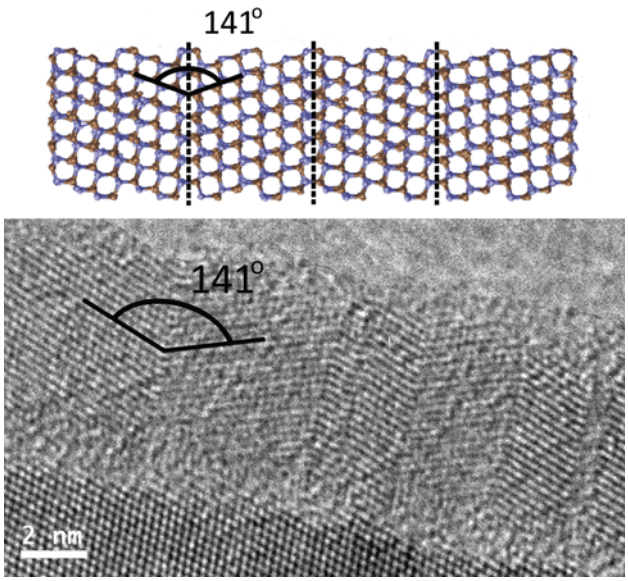

Fig. 11 TEM image of a nanowires with multiple twins. The angle subtended by crystallographic planes is 141°. Above is the atomic model of the corrugated structure of SiC nanowires caused by the twin defects, shown as *broken lines*

several adjacent crystallites. These crystallites were relatively small, 6.3 nm, and packed close to each other on the surface of the aggregate enabling SiC nanowires to grow simultaneously from several neighboring crystallites. Even thicker wires were obtained from raw N234. Here, the crystallites were smaller, 2.7 nm. Therefore, growth of SiC nanowires from a larger number of crystallites is more likely. In addition, the presence of amorphous carbon atoms on the surface of raw N234 aggregates [11] also contributed to the growth of the nanowire diameter. However, in the case of graphitized N990, the crystallites were larger, 23 nm, and no amorphous carbon has been detected [11]. Relative orientation of neighboring crystallites suddenly changes and the vectors normal to these crystallites subtends angles close or larger than 90°. Consequently, it is difficult for nanowires growing from neighboring crystallites to join together and grow as one thicker wire.

All SiC nanowires, particles, and aggregates were covered with a thin amorphous shell. The thickness of that shell was about 2 nm and did not vary substantially between the specimens. The thickness of the amorphous layer is smaller than for many nanowires produced by other techniques [23–25]. FTIR spectra show a small peak at about 1100 cm^{-1} which is attributed to the Si–O vibrations. Assuming that this broad peak is caused by vibrations of structures similar to those present in glass, we estimated concentration of SiO_2 from that peak intensity. The calculated amount accounted for about 1% of the total mass of the observed 2 nm thick film wrapping around all structures. Therefore, we concluded that the thin film on the surface of SiC nanowires and particles is mainly amorphous silicon carbide with a small amount of SiO_x. The fact that the infrared absorption peak was blue shifted further indicated that it was not pure SiO_2 but an amorphous structure of random chemical stoichiometry.

Summary

Carbon blacks reacted with silicon to form silicon carbide which coated the outer surfaces of the aggregates with a 20 nm thick layer. The shape of the aggregates was preserved. This indicates that silicon and/or silicon oxide vapor travelled toward carbon black and reacted there.

When the SiC layer coated the aggregates completely during postproduction heating in oxygen atmosphere at about 1000 K, that layer effectively blocked oxygen from reaching the interior of the particles where there was still some unreacted carbon. The structure of the interior of carbon black aggregates is a mixture of amorphous carbon and small graphitic crystallites. The small lateral sizes of these crystallites remain unchanged during the graphitization process which is limited to the outer layer of the aggregates.

Silicon carbide nanowires produced from carbon blacks formed entangled fluffy film. Individual wires were observed only under high magnification. The outer surfaces of SiC nanowires are covered with a layer of amorphous silicon carbide with traces of silicon dioxide. The thickness of that layer is about 2 nm. Morphology of the nanowires depends on carbon black grade and thermal treatment prior to the reaction with silicon. Nanowires of narrow size distribution and smooth surfaces were obtained from graphitized carbons. The use of raw carbon black N234 resulted in wires of wide distribution of sizes and included structures that appeared to be composed of irregular blocks about 5 nm in height, stacked one on the top of another. Here, concentration of twins appeared to be higher than in other nanowires. Also, nanowires of diameters that changed along the cylindrical axes were observed for raw carbon blacks, but never for graphitized carbon blacks.

We have not observed "flowers" typical for the VLS process. Also, no heavy metals were detected in SiC produced from graphitized carbons. The vapor–solid growth mechanism is more plausible than the vapor–liquid–solid mechanism.

Acknowledgement This work was partially supported by a grant NSF DMR 0502136.

References

1. Dai HJ, Wong EW, Lu YZ, Fan SS, Lieber CM (1995) Nature 375:769
2. Shim HW, Huang H (2007) Appl Phys Lett 90:083106
3. Wallis KL, Wieligor M, Zerda TW, Stelmakh S, Gierlotka S, Palosz B (2008) J Nanosci Nanotechnol 8(7):3504
4. Rich RM, Stelmakh S, Patyk J, Wieligor M, Zerda TW, Guo Q (2009) J Mater Sci 44(11):3010. doi:10.1007/s10853-009-3431-x
5. Shackelford JF, Alexander W, Park JS (eds) (1994) CRC material science and engineering handbook, 2nd edn. CRC, Boca Raton
6. Bhushan B (ed) (2007) Springer handbook of nanotechnology, 2nd edn. Springer, Berlin
7. Davis RF, Palmour JW, Edmond JA (1990) A review of the status of diamond and silicon carbide devices for high-power, -temperature, and -frequency applications. Electron devices meeting, 1990. IEDM '90. Technical Digest International, p 785–788
8. Rutter GM, Guisinger NP, Crain JN, Jarvis EA, Stiles MD, Li T, First PN, Stroscio JA (2007) Phys Rev B 76:235416
9. Guisinger NP, Rutter GM, Crain JN, First PN, Stroscio JA (2009) Nano Lett 9(4):1462
10. Berger C, Song Z, Li X, Wu X, Brown N, Naud C et al (2006) Science 312(5777):1191
11. Zerda TW, Xu W, Yang H, Gerspacher M (1998) Rubber Chem Technol 71(1):26
12. Zerda TW, Xu W, Zerda A, Zhao Y, Von Dreele RB (2000) Carbon 38(3):355
13. Xu W, Zerda TW, Yang H, Gerspacher M (1996) Carbon 34(2):165
14. Gruber T, Zerda TW, Gerspacher M (1994) Carbon 32(7):1377

15. Gruber T, Zerda TW, Gerspacher M (1994) Rubber Chem Technol 67(2):280
16. Zhang S-L, Zhu B-F, Huang F, Yan Y, Shang E, Fan S et al (1999) Solid State Commun 111(11):647
17. Zhang E, Tang Y, Zhang Y, Guo C (2009) Physica E 41:655
18. Hjelm R, Wampler W, Gerspacher M (1997) Proc SPIE 2867:144
19. Belova IV, Murch GE (2003) J Phys Chem Solids 64(5):873
20. Hon MH, Davis RF (1979) J Mater Sci 14(10):2411. doi: 10.1007/BF00737031
21. Hon MH, Davis RF, Newbury DE (1980) J Mater Sci 15(8):2073. doi:10.1007/BF00550634
22. Wieligor M, Rich R, Zerda TW (2009) APS meeting, Pittsburgh, PA, March
23. Zhang Y, Wang N, Gao S, He R, Miao S, Liu J, Zhu J, Zhang X (2002) Chem Mater 14:3564
24. Kim R, Quin W, Wei G, Wang G, Wang L, Zhang D (2009) Chem Phys Lett 1–3:86
25. Ye H, Titchenal N, Gogotsi Y, Ko F (2005) Adv Mater 2005:1531
26. Bogart TE, Dey S, Lew K, Mohney SE, Redwing JM (2005) Adv Mater 17(1):114
27. Li X, Chen X, Song H (2009) J Mater Sci 44:4661. doi: 10.1007/s10853-009-3714-2
28. Roy S, Portail M, Chassagne T, Chauveau JM, Vennegues P, Zielinski M (2009) Appl Phys Lett 95:081903
29. Niu JJ, Wang JN (2007) J Phys Chem B 111:4368
30. Davidson FM, Lee DC, Fanfair DD, Korgel BA (2007) J Phys Chem C 111:2929